Structural Engineering and Mechanics, Vol. 22, No. 6 (2006) 761-783

DOI: http://dx.doi.org/10.12989/sem.2006.22.6.761

Seismic behavior of structures isolated with a hybrid system of rubber bearings

Bo-Jen Chen†

R & D Department, Earthquake Proof Systems, Inc., Taichung, Taiwan, R.O.C.

C. S. Tsai‡

Department of Civil Engineering, Feng Chia University, Taichung, Taiwan, R.O.C.

L. L. Chung‡†

National Center for Research on Earthquake Engineering, Taipei, Taiwan, R.O.C.

Tsu-Cheng Chiang‡‡

Graduate Institute of Civil and Hydraulic Engineering, Feng Chia University, Taichung, Taiwan, R.O.C.

(Received June 17, 2004, Accepted December 21, 2005)

Abstract. The enlargement of interest in base isolators as an earthquake-proof design strategy has dramatically accelerated experimental studies of elastomeric bearings worldwide. In this paper, a new base isolator concept that is a hybrid system of rubber bearings is proposed. Uniaxial, biaxial, and triaxial shaking table tests are also performed to study the seismic behavior of a 0.4-scale three-story isolated steel structure in the National Center for Research on Earthquake Engineering in Taiwan. Experimental results demonstrate that structures with a hybrid system of rubber bearings composed of stirruped rubber bearings and laminated rubber bearings can actually decrease the seismic responses of the superstructure. It has been proved through the shaking table tests that the proposed hybrid system of rubber bearings is a very promising tool to enhance the seismic resistance of structures. Moreover, it is demonstrated that the proposed analytical model in this paper can predict the mechanical behavior of the hybrid system of rubber bearings and seismic responses of the base-isolated structures.

Keywords: rubber bearing; base isolation; seismic engineering; hybrid system.

---

† Ph.D., Assistant Research Fellow
‡ Professor, Corresponding author, E-mail: cstsai@fcu.edu.tw
‡† Division Head
‡‡ Ph.D.

1. Introduction

Base isolation is an innovative performance-based design approach to mitigate or minimize earthquake damage potential (Kelly 1997, Naeim and Kelly 1999, Komodromos 2000, Clark *et al.* 1997, Kasalanati and Constantinou 1999, Skinner *et al.* 1993). The rubber bearing systems are introduced between the superstructure and the foundation to provide lateral flexibility and energy dissipation capacity. It can not only shift the natural period of a structure away from plentiful energy-containing periods of ground motions by its low shear stiffness, but also provide considerable hysteresis damping to dissipate seismic energy that would otherwise be transmitted into structures during earthquakes. Extensive tests have been conducted on numerous different types of the rubber bearings, and applications have been found their way into many buildings and other structures in many industrialized nations.

Rubber is a complex material with polymers, fillers, oils, processing aids, accelerators, antioxidants and retarders and has the ability to deform elastically when vulcanized by sulphur. In this study, the elastomeric materials that are utilized in the manufacture of the rubber bearings consist of natural rubber, carbon black, stearic acid, activator, antioxidant, resin, softener and calcium carbonate. The experimental examinations via the component and shaking table tests, indicate that the stirruped rubber bearing possesses higher damping ratios at higher strains, and lower horizontal effective stiffness than other kinds of rubber bearings even when the vertical axial load is small (Tsai *et al.* 2002). The paper is aimed at investigating the mechanical behavior of the laminated rubber bearing (RB) and the stirruped rubber bearing (SRB) in conjunction with a series of component tests and evaluating the feasibility of the buildings equipped with the hybrid system of rubber bearings (i.e., the combinations of the laminated rubber bearings and the stirruped rubber bearings) (Tsai *et al.* 2003a). The stirruped rubber bearing (SRB) was developed by Tsai *et al.* (2002, 2003) in Taiwan, is shown in Fig. 1. In this system the cylindrical elastic material (not necessarily rubber material) was confined by a constrained stirrup so as to restrict the lateral deformation of the rubber due to axial load and increase the vertical stiffness. Besides, when lower vertical stiffness is required, it is possible to achieve this by adjusting the stirrup spacing and confining pressure (Chen *et al.* 2004). In order to understand the nonlinear mechanical behavior and earthquake-proof benefits of the laminated rubber bearings (RB) and stirruped rubber bearings (SRB), an isolator testing machine at the Feng Chia University in Taiwan was used for this study.

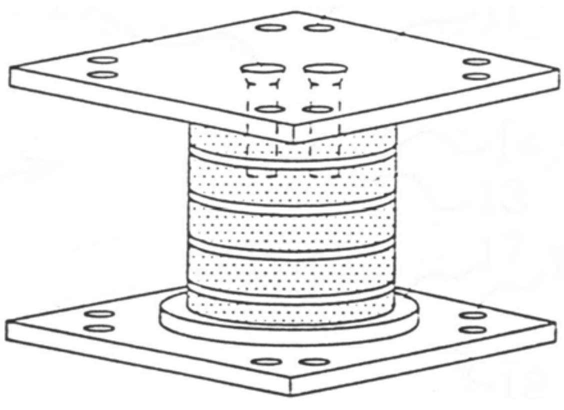

Fig. 1 Stirruped Rubber Bearing (SRB)

Besides examining the earthquake-proof benefits of buildings equipped with the hybrid system of rubber bearings, the ultimate behavior of a base-isolated structure is investigated through a series of large-scale shaking table tests of a 0.4-scale multiple-bay three-story steel frame. Uniaxial, biaxial, and triaxial shaking table tests were conducted to study the seismic responses of this 0.4-scale multiple-bay three-story isolated steel structure.

The advantages of utilizing a hybrid system of rubber bearings are as follows: (1) The stirruped rubber bearing possesses a lower horizontal effective stiffness and a higher equivalent damping ratio than the laminated rubber bearing in the same combinative rubber materials. Moreover, experimental results indicate that the stirruped rubber bearing possesses higher equivalent damping ratios at higher strains (Tsai *et al.* 2002); (2) Because the vertical stiffness of the laminated rubber bearing is higher than the stirruped rubber bearing, the laminated rubber bearings are installed at the bottoms of heavier columns (Chen *et al.* 2004); (3) The hybrid assembly of the laminated rubber bearing and stirruped rubber bearing can obtain the most outstanding horizontal earthquake-proof benefit owing to equalize the horizontal effective stiffness of each rubber bearing (Tsai *et al.* 2003a); and (4) because the stirruped rubber bearing has a three-directional earthquake-proof benefit, it can decrease the influences of the vertical ground motions on the superstructure (Tsai *et al.* 2002). Experimental results demonstrate that a structure with a hybrid system of rubber bearings can actually reduce its seismic responses.

Because of the highly nonlinear mechanical behavior of the RB and SRB as a result of its inherent damping property, many mathematical models for simulating the nonlinear mechanical properties of rubber bearings have been proposed with satisfactory accuracy (Koh and Kelly 1988, Fujita *et al.* 1990, Stanton *et al.* 1990, Tsopelas *et al.* 1991, Iizuka 1993). This paper utilizes an advanced analytical model by modifying Wen's model to adequately simulate the nonlinear mechanical behavior of the RB and SRB (Tsai *et al.* 2003b, Chen *et al.* 2001). By comparing the analytical and experimental results, it is shown that the proposed analytical model can predict the mechanical behavior of hybrid system of rubber bearings and seismic responses of the base-isolated structures.

2. Comparisons of vertical stiffnesses of rubber bearings

The approximate solution of the vertical stiffness K_v for the stirruped rubber bearing can be obtained as (Chen *et al.* 2004):

$$K_v = \frac{E_c A'}{T_r} \tag{1}$$

where

$$E_c = 3G\frac{b^2}{b^2 - a^2} + \frac{3G}{2t^2}(b^2 - a^2) \tag{2}$$

G denotes the shear modulus of the rubber material; E_c represents the effective compression modulus of the rubber bearing; A' indicates the compression area ($= \pi b^2$); t is the thickness of a single rubber layer, as shown in Fig. 2; a and b show the inner and outer radii of the stirrup, respectively; T_r denotes the total rubber layer thickness. If one assumes $a = 0$, then the effective compression modulus of the laminated rubber bearing can be given by (Kelly 1997, Naeim and Kelly 1999):

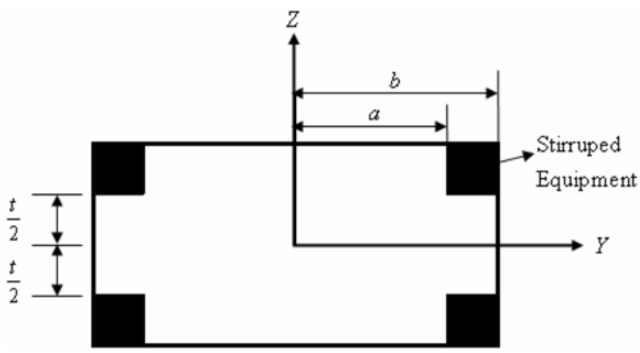

Fig. 2 Dimensions of a stirruped rubber layer

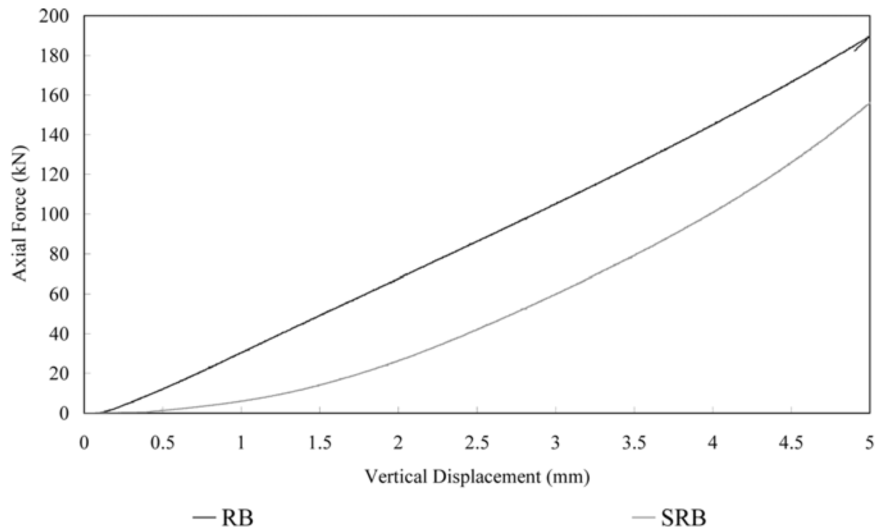

Fig. 3 Comparisons of vertical stiffnesses of RB and SRB

$$E_c = 3G + \frac{3G}{2t^2}b^2 \tag{3}$$

By comparing Eqs. (2) and (3), it is illustrated that the effective compression modulus of the stirruped rubber bearing is lower than that of the laminated rubber bearing. Fig. 3 shows the relations between the axial loads and vertical displacements for the RB and SRB. It can be seen that the vertical stiffness of the SRB is lower than the vertical stiffness of the RB.

3. Critical buckling load and design for rubber bearings

The critical buckling loads in the undeformed configuration P_{cr} for the laminated and stirruped rubber bearings are estimated by (Kelly 1997, Naeim and Kelly 1999)

$$P_{cr} = \sqrt{P_S P_E} \tag{4}$$

where

$$P_S = GA_S \tag{5}$$

$$P_E = \frac{\frac{1}{3}\pi^2 E_c I \frac{h}{T_r}}{h^2} \tag{6}$$

and

$$A_S = A'\frac{h}{T_r} \tag{7}$$

where P_S and P_E are defined as the shear stiffness per unit length and Euler buckling load for a column without shear deformation, respectively; E_c depicts the compression modulus of the stirruped rubber bearing assuming incompressible behavior; A' depicts the compressive area of the rubber bearing, being the same as the shear cross-sectional area in the design; A_S is an effective shear area to account for the fact that the steel does not deform in the composite system; h represents the total height of the rubber pads and steel shims; T_r denotes the rubber layer thickness; I illustrates the moment of inertia of a rubber bearing. With the aid of Eq. (2) to Eq. (7), the critical buckling load for the laminated and stirruped rubber bearings can be rewritten as

$$P_{cr} = \frac{N\pi^2 G\Phi^4}{32\sqrt{2}T_r^2} \quad \text{(laminated rubber bearing)} \tag{8}$$

and

$$P_{cr} = \frac{\pi^2 G b^3}{2T_r^2}\left[\frac{2T_r^2 b^2 + N^2(b^2 - a^2)^2}{2(b^2 - a^2)}\right]^{1/2} \quad \text{(stirruped rubber bearing)} \tag{9}$$

where Φ represents the diameter of the laminated rubber bearing. The parameter P_{cr}/W, the ratio of the critical buckling load to the applied load from the superstructure, can be considered as a safety factor R and the design of the rubber bearing should be such that it has a value of, say, 2 or greater. It is given as

$$R = \frac{P_{cr}}{W} \tag{10}$$

Substitution of Eq. (10) into Eqs. (8) and (9) leads to the number of rubber layers

$$N = \frac{32\sqrt{2}RWT_r^2}{\pi^2 G\Phi^4} \quad \text{(laminated rubber bearing)} \tag{11}$$

and

$$N = \left[\frac{8R^2W^2T_r^4}{\pi^4 G^2 b^6(b^2 - a^2)} - \frac{2T_r^2 b^2}{(b^2 - a^2)^2}\right]^{1/2} \quad \text{(stirruped rubber bearing)} \tag{12}$$

Then the thickness of a single-layer of rubber can be given by

$$t_r = \frac{T_r}{N} \tag{13}$$

The total height of the stirruped rubber bearing is

$$H = T_r + (N-1)t_s + T \tag{14}$$

where T, T_r and t_s denote end plates thickness, rubber layers thickness and single steel ring thickness, respectively.

4. An analytical model for rubber bearings

To adequately predict the non-linear behavior of a hybrid system of rubber bearings under strong ground motions, the revised Wen's model was given by (Tsai *et al.* 2003b, Chen *et al.* 2001, Wen 1976, Tsopelas *et al.* 1994):

$$dF_i(t) = \alpha\frac{F^y}{Y}dU_i(t) + (1-\alpha)F^y dZ_i(t), \quad i = \zeta, \eta \tag{15}$$

and

$$dZ_i(t)Y = AdU_i(t) - Z_i^N(t)Q_i(t)dU_i(t), \quad i = \zeta, \eta \tag{16}$$

where

$$Q_i(t) = \gamma\mathrm{sgn}(dU_i(t)\cdot Z_i(t)) + \beta, \quad i = \zeta, \eta \tag{17}$$

in which ζ and η denote the local coordinate system, as shown in Fig. 4; α indicates the ratio of the post-yielding to the pre-yielding stiffness. F^y and Y represent the yield force and the yield displacement, respectively; $dU_i(t)$ is the displacement increment in the i direction; $Z_i(t)$ denote the dimensionless variable that controls plastic behavior in the i direction; A, γ and β are dimensionless quantities that control the shape of the hysteresis loop. Kasalanati and Constantinou (1999) have

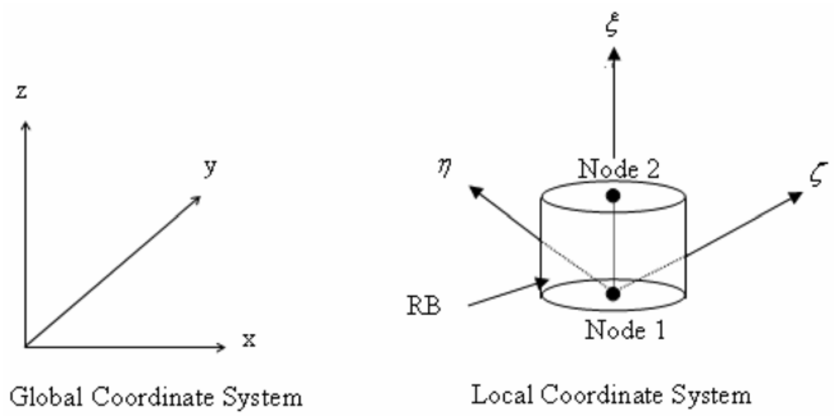

Fig. 4 Two-node base isolation element

proposed that $A/(\beta+\gamma) = 1$. In particular, $A = 1$, $\beta = 0.1$ and $\gamma = 0.9$ are suggested. If $N = 2$, the following second-order polynomial equation for $dZ_i(t)$ can be obtained by substituting $Z_i(t) = Z_{pi}(t) + dZ_i(t)$ into Eq. (5)

$$dZ_i^2(t) + \left(\frac{Y}{Q_i(t)dU_i(t)} + 2Z_{pi}(t)\right)dZ_i(t) + \left(Z_{pi}^2(t) - \frac{A}{Q_i(t)}\right) = 0, \quad i = \zeta, \eta \tag{18}$$

where $Z_{pi}(t)$ depicts the known Z value of the previous time step. From Eq. (18), the exact solution of $dZ_i(t)$ can be easily obtained as follows:

$$dZ_i(t) = \frac{1}{2}\left\{-\left(\frac{Y}{Q_i(t)dU_i(t)} + 2Z_{pi}(t)\right) \pm \sqrt{\left(\frac{Y}{Q_i(t)dU_i(t)} + 2Z_{pi}(t)\right)^2 - 4\left(Z_{pi}^2(t) - \frac{A}{Q_i(t)}\right)}\right\} \tag{19}$$

Because the rubber bearing behavior shows velocity dependence with an elliptical shape at small shear strains, the horizontal force F should be a summation of the forces F_s (displacement dependent shear force) and F_v (velocity dependent shear force), and is given as (Chen *et al.* 2001, Wen 1976)

$$\begin{aligned} F_i(t) &= F_{si}(t) + F_{vi}(t) = F_{si}(t-\Delta t) + dF_{si}(t) + F_{vi}(t) \\ &= F_{si}(t-\Delta t) + D_i(t)dU_i(t) + C_i(t)\dot{U}_i(t), \quad i = \zeta, \eta \end{aligned} \tag{20}$$

where

$$D_i(t) = \frac{F^y}{Y}[\alpha + (1-\alpha)(A - Z_i^2(t)Q_i(t))], \quad i = \zeta, \eta \tag{21}$$

$D(t)$ represents the stiffness of rubber bearings in the horizontal direction; $C(t)$ depicts the viscous damping coefficient.

5. Component tests of rubber bearings

In order to understand the behavior of an isolator system, isolators need to undergo rigorous laboratory testing. The conditions under which the testing should be done include a wide range of axial loads, displacements and frequencies. Isolators exhibit changes in height when laterally displaced. Thus, an isolator testing machine should be able to maintain the desired vertical load on the bearing during these movements. The test setup is capable of making bearings to sustain horizontal and vertical loads at same time. Fig. 5 shows that the type of laminated rubber bearing (noted as RB) tested is 146 mm in diameter and 84 mm in height. They consist of 10 rubber layers of 5 mm thickness each, 9 steel plates of 1mm thickness each and 3 mm rubber cover, and each end plate is 12.5 mm thick with bolted connections. Fig. 6 shows that the stirruped rubber bearing (noted as SRB) tested is also 146 mm in diameter and 84 mm in height. Each bearing consists of a layer of rubber material 54 mm in thickness, 4 external steel rings of 6 mm thickness, 3 mm rubber cover, and a plate of 15 mm thickness with bolted connections at each end.

Figs. 7 and 8 represent the comparisons of the horizontal effective stiffness and equivalent damping ratio trends of the RB while the test horizontal frequency of 0.5 Hz, and the axial load of

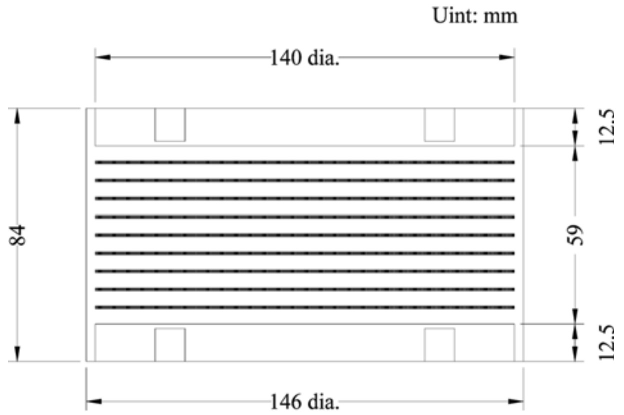

Fig. 5 Schematic of cylindrical laminated rubber bearing (RB)

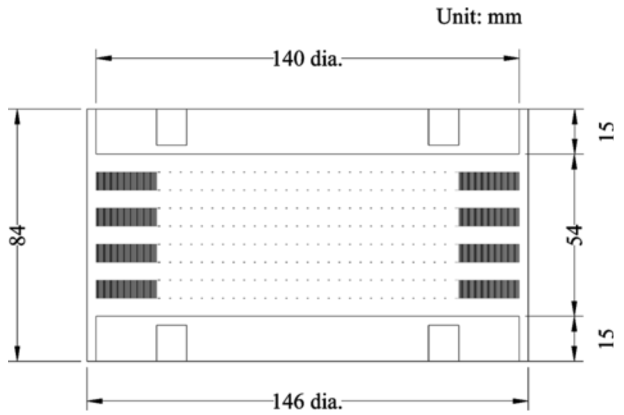

Fig. 6 Schematic of cylindrical partially confined stirruped rubber bearing (SRB)

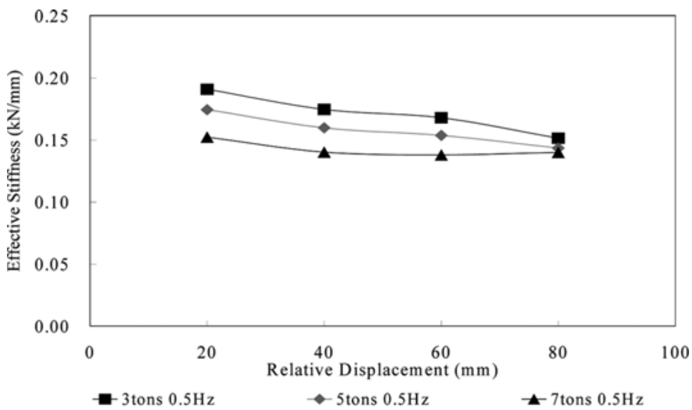

Fig. 7 Horizontal effective stiffness of RB of 140 mm in diameter (Axial Load = 3, 5, 7 tons, Frequency = 0.5 Hz)

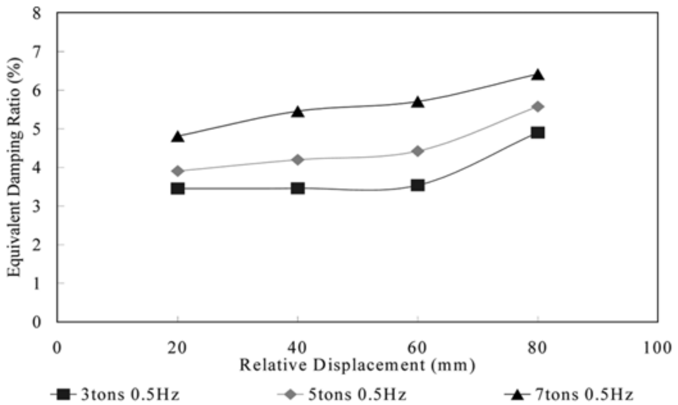

Fig. 8 Equivalent damping ratio of RB of 140 mm in diameter (Axial Load = 3, 5, 7 tons, Frequency = 0.5 Hz)

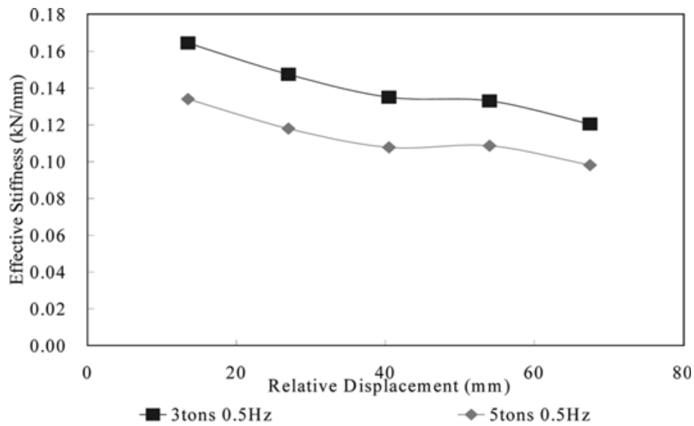

Fig. 9 Horizontal effective stiffness of SRB of 140 mm in diameter (Axial Load = 3, 5 tons, Frequency = 0.5 Hz)

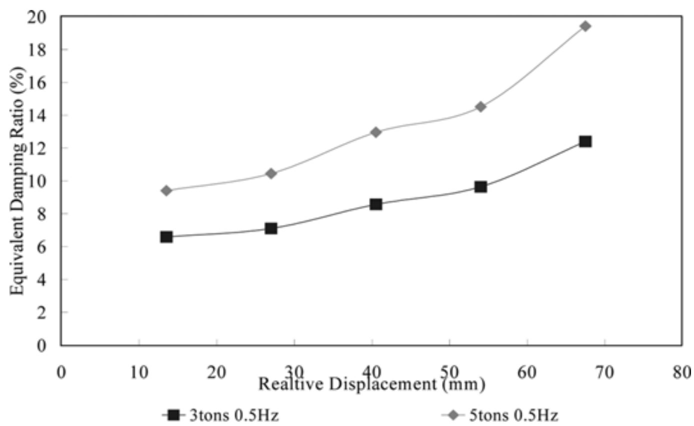

Fig. 10 Equivalent damping ratio of SRB of 140 mm in diameter (Axial Load = 3, 5 tons, Frequency = 0.5 Hz)

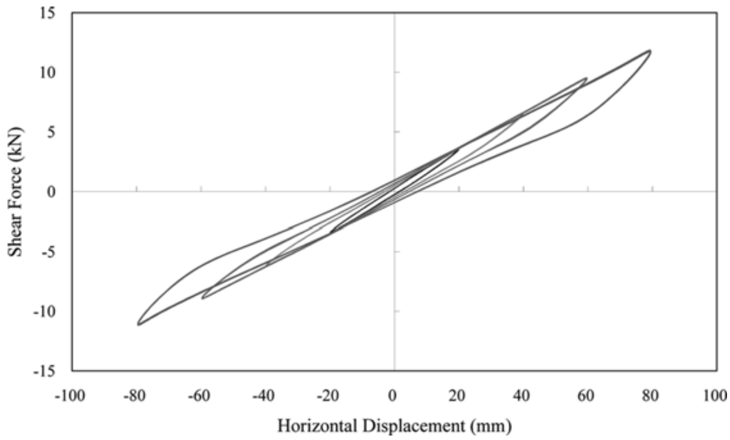

Fig. 11 Experimental result of laminated rubber bearing at an axial load of 5 tons and frequency of 0.5 Hz

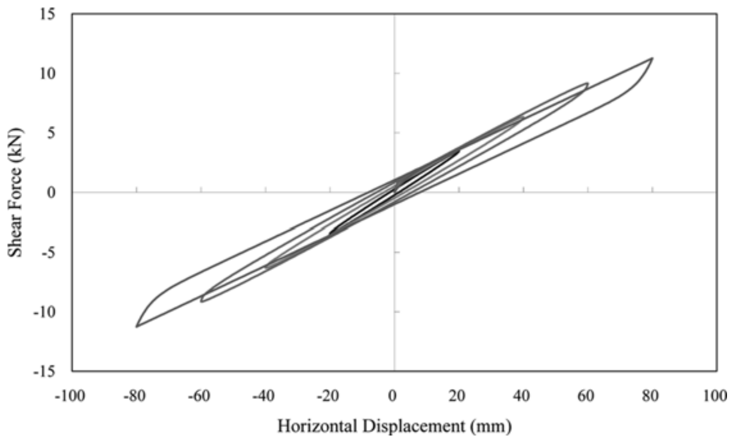

Fig. 12 Analytical result of laminated rubber bearing at an axial load of 5 tons and frequency of 0.5 Hz

3 tons, 5 tons and 7 tons are applied. Figs. 9 and 10 represent the comparisons of the horizontal effective stiffness and equivalent damping ratio trends of the SRB while the test horizontal frequency of 0.5 Hz, and the axial load of 3 tons and 5 tons are applied. From Figs. 7 to 10, it can be seen that the experimental results show a significant decrease in the horizontal effective stiffness and a remarkable increase in the equivalent damping ratio with increasing axial loads. Moreover, the experimental results show that the SRB possesses a lower horizontal effective stiffness and a higher equivalent damping ratio than the RB.

In this paper, to demonstrate the accuracy of the proposed analytical model for the RB and SRB, the results obtained from the analytical model were compared with the experimental results of the component tests. Figs. 11 and 12 display the comparisons of the analytical and experimental results for the RB with an axial load of 5 tons and the test frequency of 0.5 Hz at different horizontal displacements. Figs. 13 and 14 show the comparisons of the analytical and experimental results for the SRB while an axial load of 3 tons and test frequency of 0.5 Hz are applied. Figs. 11 to 14 illustrate that the proposed theoretical model can well predict the dynamic mechanical behavior of

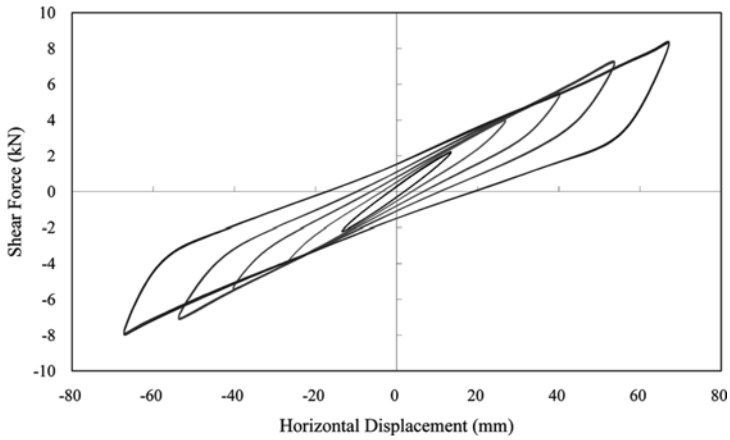

Fig. 13 Experimental result of stirruped rubber bearing at an axial load of 3 tons and frequency of 0.5 Hz

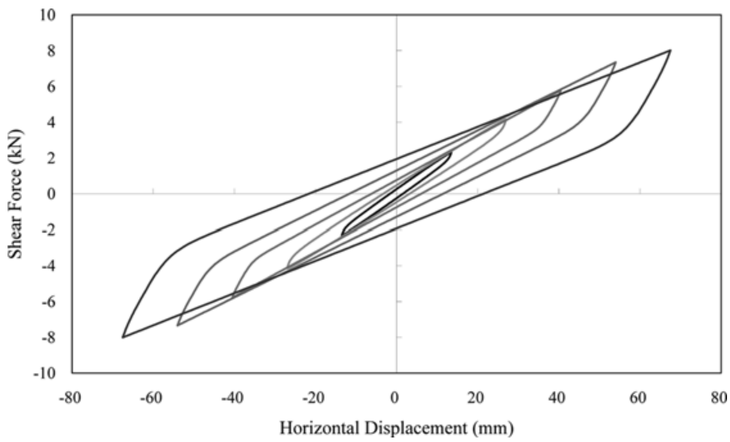

Fig. 14 Analytical result of stirruped rubber bearing at an axial load of 3 tons and frequency of 0.5 Hz

the RB and SRB. The used parameters calculating to mechanical properties of the RB and SRB at different horizontal relative displacement are shown in Tables 1 and 2.

Table 1 Parameters of numerical analyses for laminated rubber bearing at an axial load of 5 tons and frequency of 0.5 Hz

	F^y (kN)	Y (mm)	A	α	β	γ	N	C (kN×sec/mm)
20 mm	0.05	8.00	1.0	0.43	0.1	0.9	0.1	0.0035
40 mm	0.10	4.00	1.0	0.39	0.1	0.9	0.2	0.0035
60 mm	0.40	1.00	1.0	0.37	0.1	0.9	0.2	0.0030
80 mm	1.50	0.27	1.0	0.32	0.1	0.9	2.0	0

Table 2 Parameters of numerical analyses for stirruped rubber bearing at an axial load of 3 tons and frequency of 0.5 Hz

	F^y (kN)	Y (mm)	A	α	β	γ	N	C (kN×sec/mm)
13.5 mm	0.25	1.60	1.0	0.40	0.1	0.9	0.6	0.0025
27.0 mm	0.40	1.00	1.0	0.36	0.1	0.9	0.6	0.0025
40.5 mm	1.10	0.36	1.0	0.31	0.1	0.9	2.0	0
54.0 mm	1.80	0.22	1.0	0.28	0.1	0.9	2.0	0
67.5 mm	2.50	0.16	1.0	0.23	0.1	0.9	2.0	0

6. Shaking table tests of a multiple-bay isolated structure

In order to verify the earthquake-proof benefits of the hybrid system of rubber bearings, a series of shaking table tests of a multiple-bay isolated structure with hybrid system of rubber bearings were carried out in the National Center for Research on Earthquake Engineering in Taiwan. As shown in Figs. 15 to 17, a 40% scale three-story base-isolated steel structure is constructed as a moment-resisting frame. The structure used for mounting base isolators is rectangular in shape, rising 4.25 m vertically and occupying a plane of 4.5 m × 4 m horizontally. The weights of the floors from the base to the roof were approximately equal to 108, 93, 93, and 85 kN, respectively. The base-isolated structure was subjected to the 1940 El Centro earthquake, 1952 Taft earthquake, 1989 Loma Prieta (Corralitos) earthquake, 1994 Northridge (New Hall) earthquake in U.S.A., and the 1999 Chi-Chi (TCU129) earthquake in Taiwan. The fixed-base and base-isolated conditions of the model were tested using random white noises to determine their natural frequencies. The first

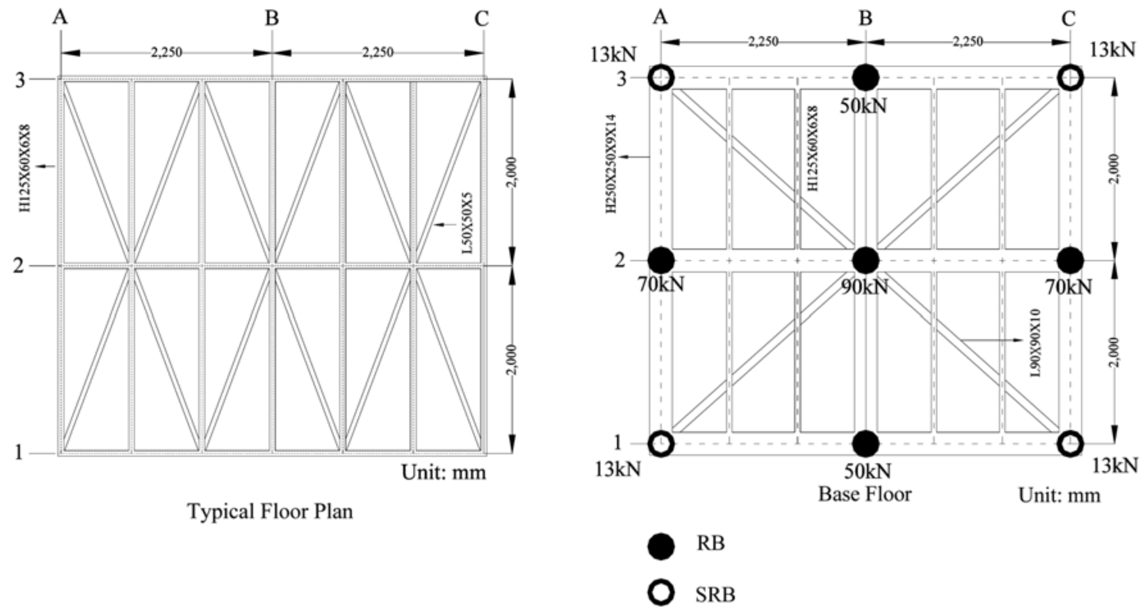

Fig. 15 Typical plan of base-isolated structure tested

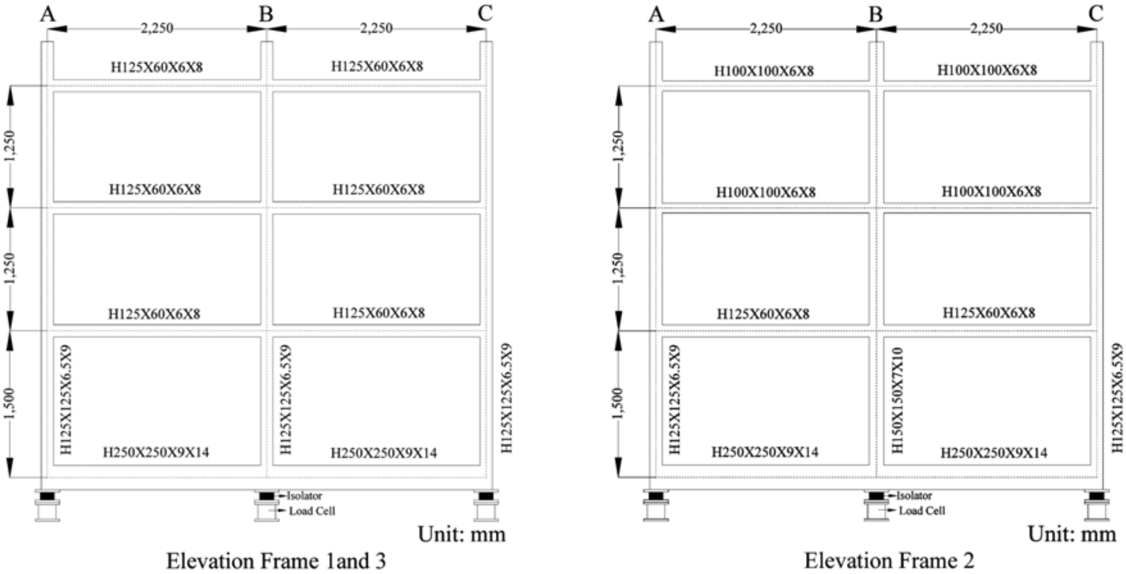

Fig. 16 Longitudinal direction elevation of base-isolated structure tested

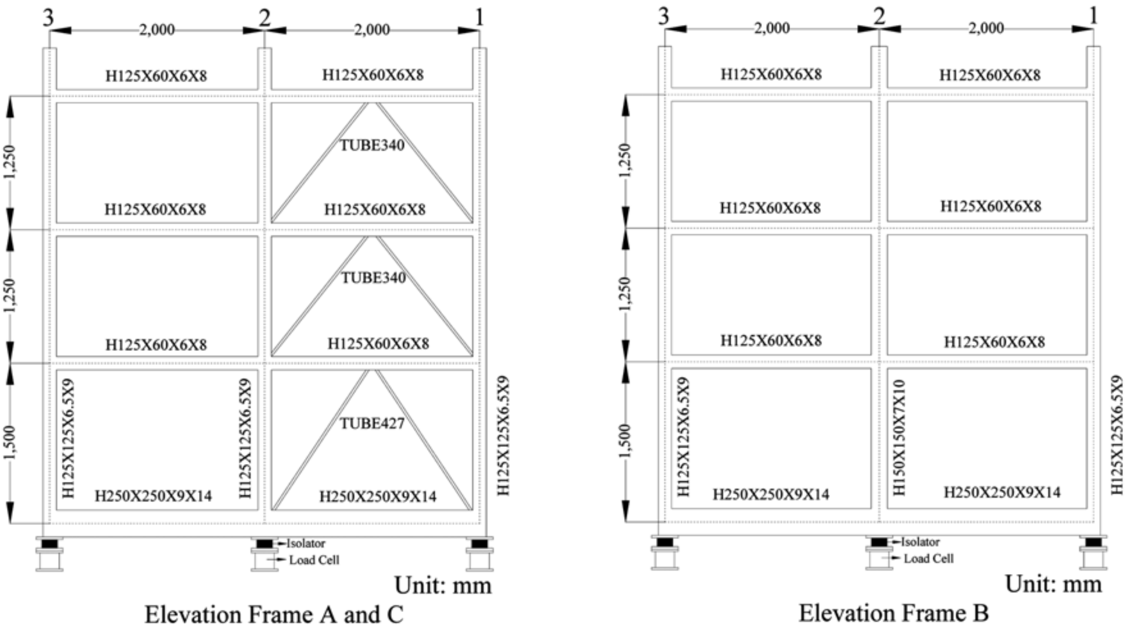

Fig. 17 Transverse direction elevation of base-isolated structure tested

two natural frequencies for the fixed-base structure are 2.91 Hz and 11.91 Hz in the longitudinal (X) direction, 4.69 Hz and 14.84 Hz in the transverse (Y) direction, and 14.65 Hz and 29.32 Hz in the vertical (Z) direction. For the base-isolated condition, the first mode natural frequencies are 1.17 Hz, 1.25 Hz and 11.72 Hz in the longitudinal (X), transverse (Y) and vertical (Z) directions, respectively.

Table 3 Comparisons of bare frame to structure isolated with hybrid system of rubber bearings in absolute acceleration responses of roof under uniaxial earthquakes

	Bare frame	With isolators	Reduction factor
Chi-Chi, X 1.022 g	2.371 g	0.446 g	81%
Chi-Chi, Y 1.096 g	3.100 g	0.355 g	89%
El Centro, X 0.601 g	2.563 g	0.410 g	84%
El Centro, Y 0.329 g	1.279 g	0.391 g	69%
Loma Prieta, X 1.027 g	1.969 g	0.423 g	79%
Loma Prieta, Y 0.500 g	1.560 g	0.353 g	77%
Northridge, X 0.317 g	0.934 g	0.322 g	66%
Northridge, Y 0.311 g	2.026 g	0.292 g	86%
Taft, X 0.555 g	1.311 g	0.332 g	75%
Taft, Y 0.390 g	2.086 g	0.380 g	82%

Table 4 Comparisons of bare frame to structure isolated with hybrid system of rubber bearings in absolute acceleration responses of roof under biaxial and triaxial earthquakes

	Bare frame	With isolators	Reduction factor
Chi-Chi X 1.200 g +Y 0.565 g	X 2.912 g Y 1.641 g	X 0.534 g Y 0.202 g	X 82% Y 88%
Chi-Chi X 0.900 g + Y 0.479 g + Z 0.238 g	X 2.011 g Y 1.418 g	X 0.417 g Y 0.185 g	X 79% Y 87%
El Centro X 0.470 g +Y 0.329 g	X 2.063 g Y 1.300 g	X 0.313 g Y 0.344 g	X 85% Y 74%
El Centro X 0.323 g +Y 0.203 g + Z 0.195 g	X 1.469 g Y 1.000 g	X 0.244 g Y 0.254 g	X 83% Y 75%
Loma Prieta X 0.672 g + Y 0.466 g	X 1.563 g Y 1.459 g	X 0.291 g Y 0.328 g	X 81% Y 78%
Loma Prieta X 0.634 g + Y 0.468 g + Z 0.377 g	X 1.435 g Y 1.481 g	X 0.339 g Y 0.351 g	X 76% Y 76%
Northridge X 0.202 g + Y 0.206 g	X 0.805 g Y 1.340 g	X 0.214 g Y 0.187 g	X 73% Y 86%
Northridge X 0.201 g + Y 0.206 g + Z 0.197 g	X 0.708 g Y 1.522 g	X 0.322 g Y 0.203 g	X 55% Y 87%
Taft X 0.244 g + Y 0.297 g	X 0.733 g Y 1.593 g	X 0.159 g Y 0.320 g	X 78% Y 80%
Taft X 0.248 g + Y 0.292 g + Z 0.208 g	X 0.919 g Y 1.550 g	X 0.223 g Y 0.338 g	X 76% Y 78%

The comparisons of the roof absolute acceleration responses of the structure with and without hybrid system of rubber bearings under different uniaxial, biaxial and triaxial ground motions are shown in Tables 3 and 4, respectively. The significant reductions of structural responses shown in Tables 3 and 4 demonstrate that the structure with a hybrid system of rubber bearings can lessen the

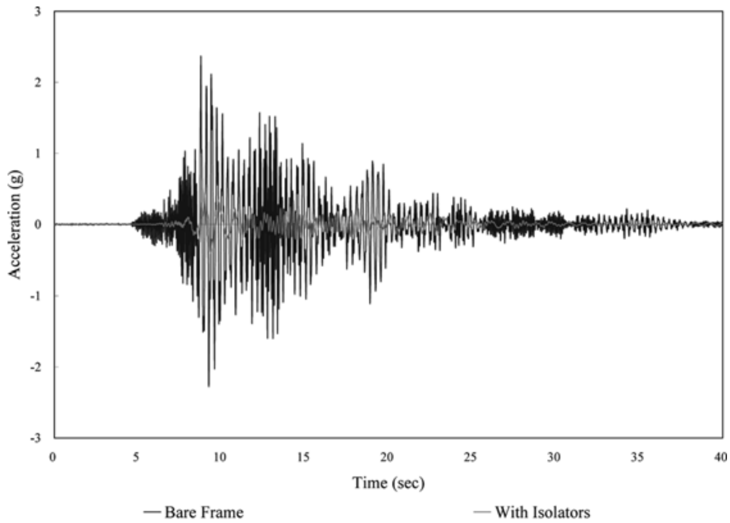

Fig. 18 Absolute longitudinal accelerations of roof for multiple-bay structure with and without hybrid system of rubber bearings under Chi-Chi (TCU129) uniaxial earthquake (PGA=1.022 g)

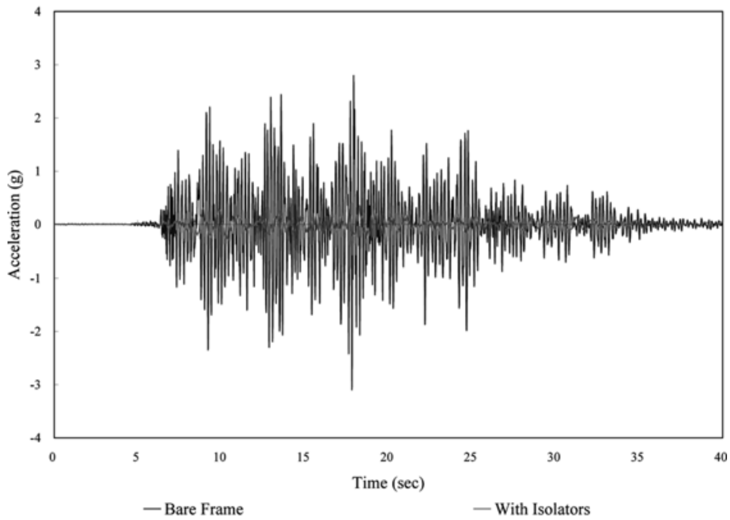

Fig. 19 Absolute transverse accelerations of roof for multiple-bay structure with and without hybrid system of rubber bearings under Chi-Chi (TCU129) uniaxial earthquake (PGA=1.096 g)

seismic responses of the superstructure. Figs. 18 and 19 display the absolute longitudinal and transverse accelerations respectively of the roof of the multiple-bay structure with and without hybrid system of rubber bearings during the Chi-Chi (TCU129) earthquake ground motions. Figs. 20 and 21 portray the absolute roof accelerations in the longitudinal and transverse directions respectively of the multiple-bay structure with and without hybrid system of rubber bearings during the El Centro earthquake. It is demonstrated that the multiple-bay structure with hybrid system of

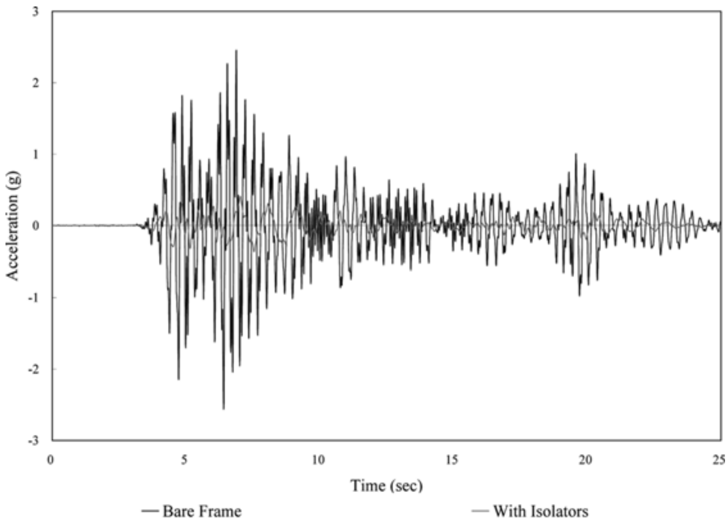

Fig. 20 Absolute longitudinal accelerations of roof for multiple-bay structure with and without hybrid system of rubber bearings under El Centro uniaxial earthquake (PGA=0.601 g)

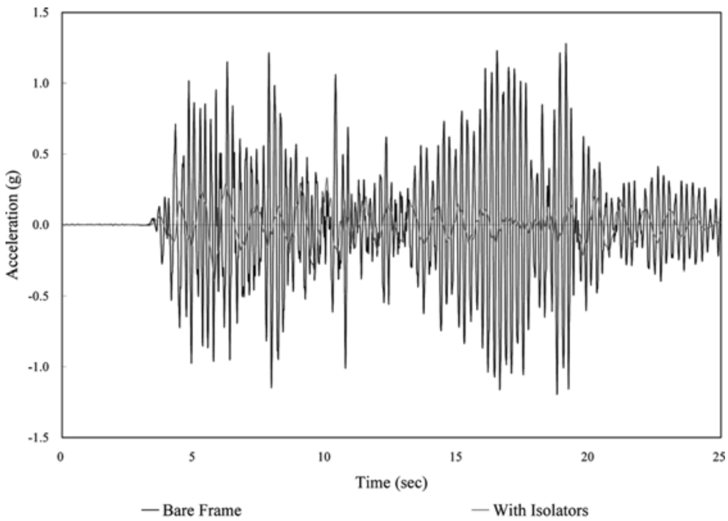

Fig. 21 Absolute transverse accelerations of roof for multiple-bay structure with and without hybrid system of rubber bearings under El Centro uniaxial earthquake (PGA=0.329 g)

rubber bearings can significantly curtail the seismic responses of the superstructure. Figs. 22 to 25 represent the comparisons of the absolute acceleration envelopes at each story between the structure with and without a hybrid system of rubber bearings under different ground motions. Figs. 22 and 23 indicate the peak absolute acceleration envelopes in the longitudinal direction of the multiple-bay structure. The peak absolute acceleration envelopes in the transverse direction of the multiple-bay structure are shown in Figs. 24 and 25. It is observed that the peak absolute accelerations with the hybrid system of rubber bearings are much smaller than those without a hybrid system of rubber bearings.

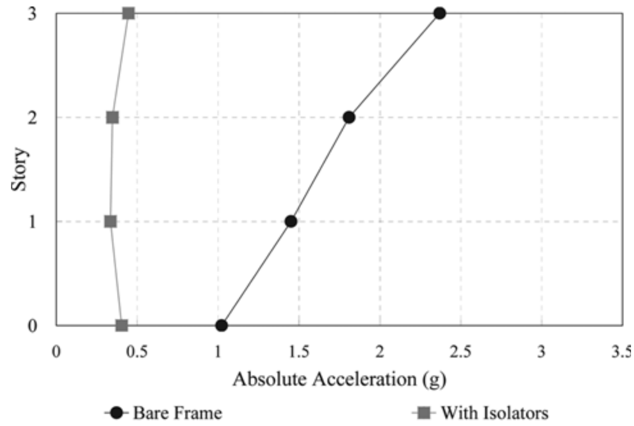

Fig. 22 Absolute longitudinal accelerations envelopes of multiple-bay structure (Chi-Chi (TCU129) uniaxial earthquake, X 1.022 g)

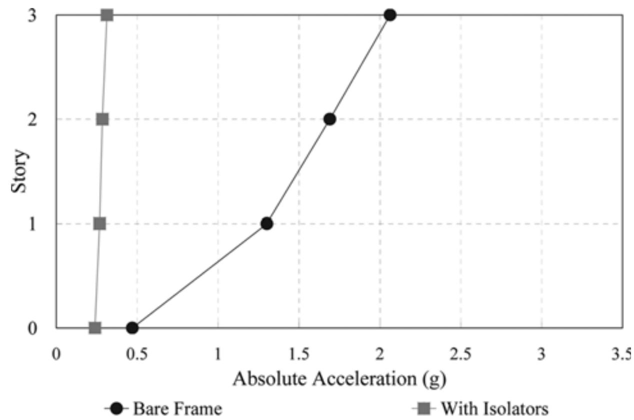

Fig. 23 Absolute longitudinal accelerations envelopes of multiple-bay structure (El Centro biaxial earthquake, X 0.470 g + Y 0.329 g)

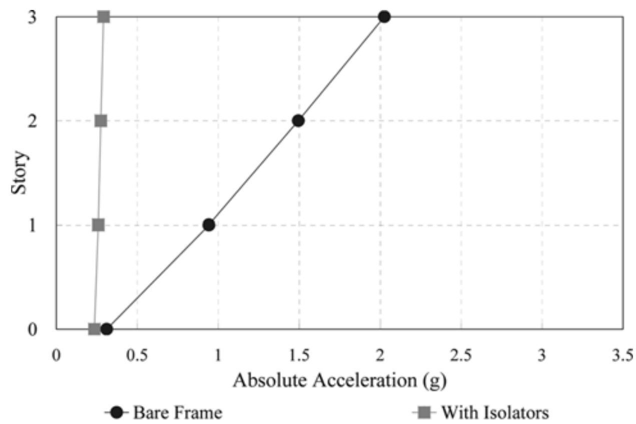

Fig. 24 Absolute transverse accelerations envelopes of multiple-bay structure (Northridge (New Hall) uniaxial earthquake, Y 0.311 g)

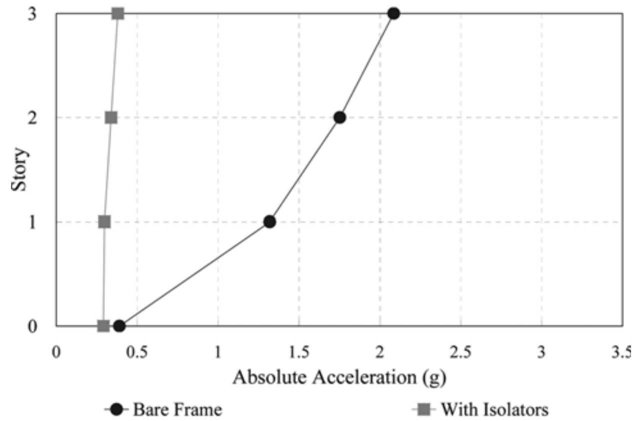

Fig. 25 Absolute transverse accelerations envelopes of multiple-bay structure (Taft uniaxial earthquake, Y 0.390 g)

In this paper, an advanced analytical model for rubber bearings was used to predict the behavior of the multiple-bay structure with a hybrid system of rubber bearings. The NSAT program was utilized to analyze the nonlinear behavior of the multiple-bay structure with hybrid system of rubber bearings (Tsai 1996). The parameters for the numerical analyses are $F^y = 1.5$ kN, $Y = 0.27$ mm, $\alpha = 0.4$, $\beta = 0.10$, $\gamma = 0.90$, $A = 1$, $N = 2$ and $C = 0$ kN × sec/mm. As shown in Figs. 26 and 27, the seismic responses of the multiple-bay structure with a hybrid system of rubber bearings can be simulated with reasonable agreement. Fig. 28 shows the analytical and experimental results of the hysteresis loops of the hybrid system of rubber bearings in the longitudinal direction of the isolated structure during the Chi-Chi (TCU129) earthquake (X 1.022 g). It is also illustrated that the mechanical behavior of the hybrid system of rubber bearings can be also simulated with close agreement.

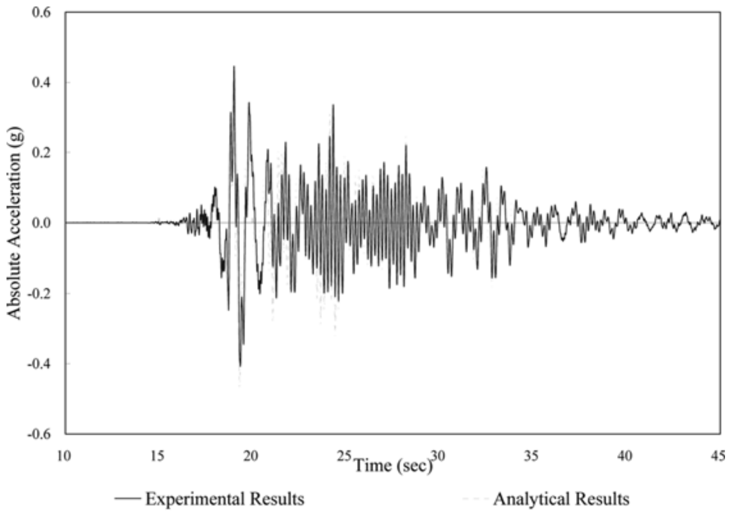

Fig. 26 Analytical and experimental results of roof absolute accelerations in longitudinal direction of multiple-bay structure with hybrid system of rubber bearings (Chi-Chi (TCU129) uniaxial earthquake, X 1.022 g)

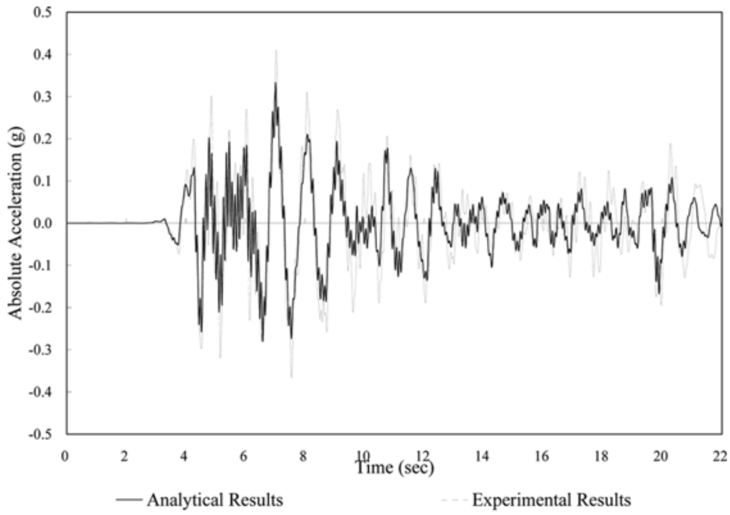

Fig. 27 Analytical and experimental results of roof absolute accelerations in longitudinal direction of multiple-bay structure with hybrid system of rubber bearings (El Centro uniaxial earthquake, X 0.601 g)

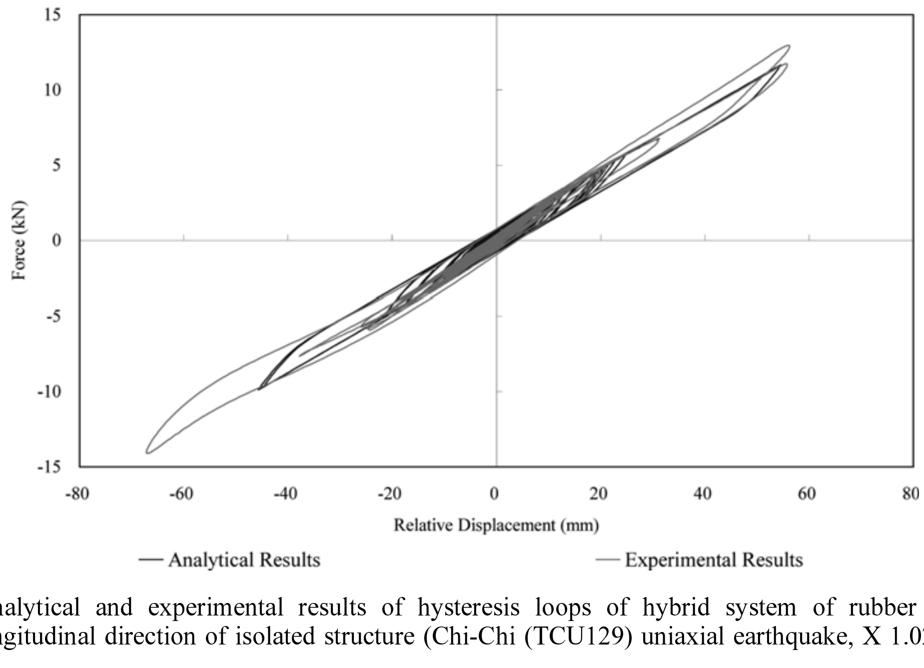

Fig. 28 Analytical and experimental results of hysteresis loops of hybrid system of rubber bearings in longitudinal direction of isolated structure (Chi-Chi (TCU129) uniaxial earthquake, X 1.022 g)

In order to demonstrate the vertical direction earthquake-proof benefits of the hybrid system of rubber bearings, the another layout of the base isolators for the shaking table tests is shown as Fig. 29. Fig. 30 is the vertical absolute acceleration response of the roof of the scaled-down steel structure with and without the laminated rubber bearings (RB) during the triaxial El Centro (X 0.332 g + Y 0.200 g + Z 0.287 g) earthquake, the vertical absolute acceleration response is slightly lessened from 0.596 g to 0.454 g (24% reduction). Fig. 31 displays the vertical absolute acceleration

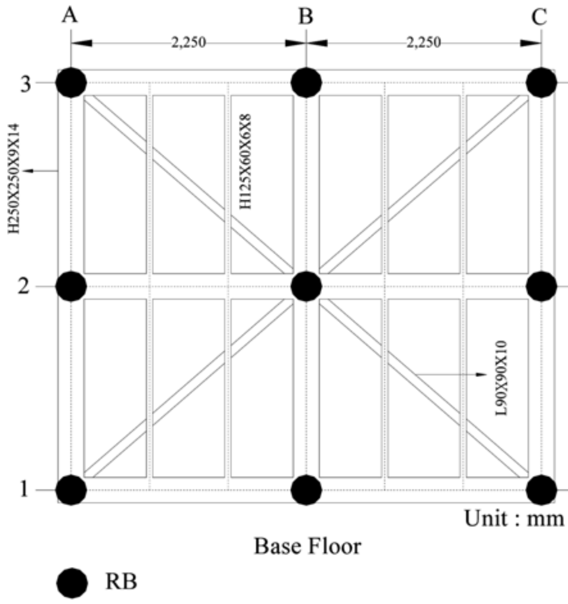

Fig. 29 Layout of laminated rubber bearings

response of the roof of the scaled-down steel structure with and without the hybrid system of rubber bearings (RB + SRB) during the triaxial El Centro (X 0.323 g + Y 0.203 g + Z 0.195 g) earthquake ground motions, the vertical absolute acceleration response is reduced from 0.404 g to 0.233 g (42% reduction). By comparing the Figs. 30 and 31, the vertical earthquake-proof benefit of the scaled-down steel structure with the hybrid system of rubber bearings is better than that with the laminated

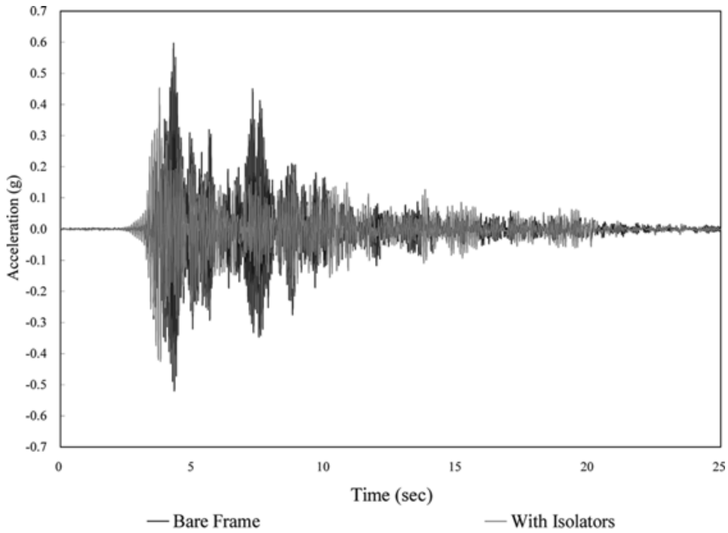

Fig. 30 Vertical acceleration responses of roof for steel frame with and without laminated rubber bearings during triaxial El Centro earthquake (X 0.332 g + Y 0.200 g + Z 0.287 g)

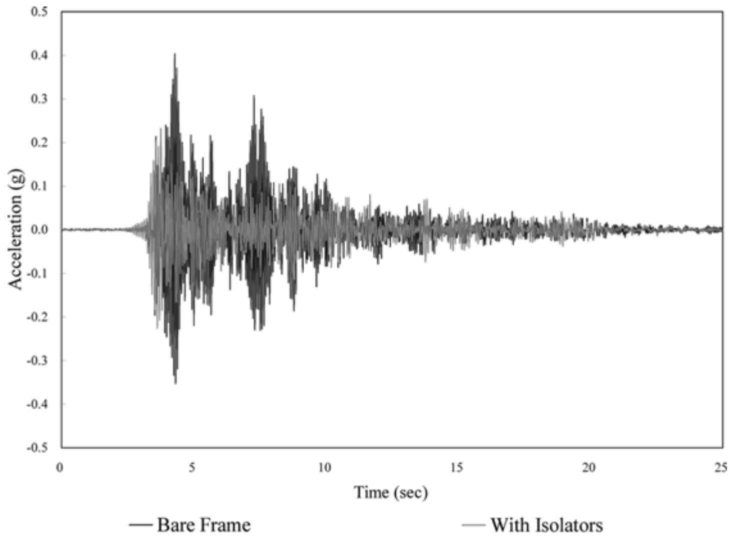

Fig. 31 Vertical acceleration responses of roof for steel frame with and without hybrid system of rubber bearings during triaxial El Centro earthquake (X 0.323 g + Y 0.203 g + Z 0.195 g)

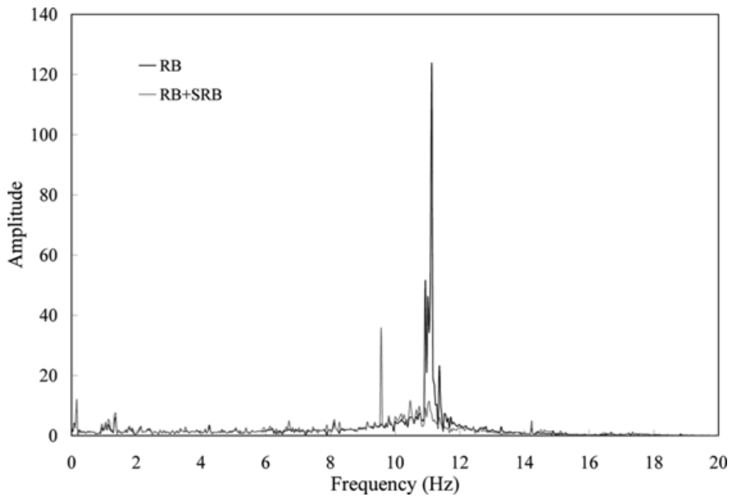

Fig. 32 Fourier transform of vertical acceleration histories of roof with laminated rubber bearings and hybrid system of rubber bearings during El Centro earthquake

rubber bearings. Fig. 32 represents the Fourier Transform of the vertical acceleration histories of the roof with the laminated rubber bearings, and with the hybrid system of rubber bearings under the triaxial El Centro earthquake ground motions. It is shown that the vertical vibration frequencies of the scaled-down steel structure with the hybrid system of rubber bearings are lower than that with the laminated rubber bearings during the earthquake ground motions. The vertical vibration frequencies of the scaled-down steel structure with the hybrid system of rubber bearings and the laminated rubber bearings are 9.57 Hz and 11.13 Hz, respectively. The vertical frequency content of the input El Centro earthquake is 13.48 Hz. It is shown that the vertical natural frequency of the structure with the hybrid system of rubber bearings is far away from the vertical frequency band of the input ground motions. Besides, the stirruped rubber bearing possesses a higher equivalent damping ratio than the laminated rubber bearing. It can further decrease the vertical vibration responses of the superstructure. It is also shown that the structure with hybrid system of rubber bearings can actually lessen the vertical absolute acceleration responses of the superstructure.

7. Conclusions

Seismic isolation is an alternative approach for seismic mitigation for relatively high-frequency structures, especially in low- to medium-rise buildings. In this study, the hybrid system of rubber bearings installed in a multiple-bay structure can shift the fundamental period of the base-isolated structure to a value beyond the range of the high energy-containing periods of earthquake motions, and supplies significant damping to dissipate energy caused by these motions. Experimental results demonstrate that structures with a hybrid system of rubber bearings can significantly decrease the horizontal seismic responses of the superstructure. Besides, it has also been demonstrated that the hybrid system of rubber bearings possesses vertical direction earthquake-proof benefits through the tri-axial shaking table tests of the scaled-down isolated structure. The proposed analytical model obtained by modifying the Wen's model can adequately simulate the nonlinear mechanical behavior of the laminated and stirruped rubber bearings. By comparing the analytical and experimental results, it is illustrated that the proposed analytical model can well predict the seismic responses of base-isolated structures.

Acknowledgements

The authors are grateful to the support for this study provided by the National Science Council, Taiwan, (NSC 90-2211-E-035-016). The assistance form the National Center for Research on Earthquake Engineering in Taiwan is appreciated.

References

Chen, B.J., Lin, S.B. and Tsai, C.S. (2001), "Theoretical and experimental study of high damping rubber bearings", *Seismic Engineering 2001, The 2001 ASME PVP Conf.*, Vol. 2, Edited by G. Roussel, Atlanta, Georgia, U.S.A., 155-162.

Chen, B.J., Tsai, C.S. and Chiang, T.C. (2004), "Compressive stiffness verification of stirrup rubber bearing", *Seismic Engineering 2004, The 2004 ASME PVP Conf.*, Edited by V.C. Matzen and S. Fujita, San Diego, California, U.S.A., July 25-29, **1**, 217-224.

Clark, Peter W., Aiken, Ian D. and Kelly, James M. (1997), "Experimental studies of the ultimate behavior of seismically-isolated structures", Technical Report EERC-97-18, Earthquake Engineering Research Center, University of California · Berkeley, California, U.S.A.

Fujita, T., Suzuki, S. and Fujita, S. (1990), "High damping rubber bearings for seismic isolation of buildings", *Trans. Japan Soc. Mech. Eng.*, **C56**, 658-666.

Iizuka, M. (1993), *Recommendation for the Design of Base Isolated Buildings*, Architectural Institute of Japan.

Kasalanati, Amarnath and Constantinou, Michael C. (1999), "Experimental study of bridge elastomeric and other isolation and energy dissipation systems with emphasis on uplift prevention and high velocity near-source seismic excitation", Technical Report MCEER-99-0004, University at Buffalo, State University of New York, U.S.A.

Kelly, J.M. (1997), *Earthquake-Resistant Design with Rubber*, Second Edition, London.

Koh, C.G. and Kelly, J.M. (1988), "A simple mechanical model for elastomeric bearings used in base isolation", *Int. J. Mech. Sci.*, **30**(12), 933-943.

Komodromos, Petros (2000), *Seismic Isolation for Earthquake-Resistant Structures*, WIT Press, Ashurst Lodge, Ashurst, Southampton, SO40 7AA, UK.

Naeim, F. and Kelly, J.M. (1999), *Design of Seismic Isolated Structures-From Theory to Practice*, John Wiley & Sons, Inc..

Skinner, R.I., Robinson, W.H. and McVerry, G.H. (1993), *An Introduction to Seismic Isolation*, John Wiley & Sons, Inc..

Stanton, J.F., Scroggings, G., Taylor, A.W. and Roeder, C.W. (1990), "Stability of laminated elastomeric bearings", *J. Eng. Mech.*, **116**(6), 1351-1371.

Tsai, C.S. (1996), "Nonlinear stress analysis techniques.-NSAT", Department of Civil Engineering, Feng Chia University, Taichung, Taiwan, R.O.C..

Tsai, C.S., Chen, B.J. and Chiang, T.C. (2002), "Shaking table tests of full scale base-isolated structures", *Seismic Engineering 2002, The 2002 ASME PVP Conf.,* Vol. 2, Edited by S.C. Lu, Vancouver, British Columbia, Canada, 245-252.

Tsai, C.S., Chen, B.J., Chiang, T.C. and Lee, G.H. (2003a), "Experimental study of a multiple bay structure isolated with hybrid bearings", *Seismic Engineering 2003, The 2003 ASME PVP Conf.*, Edited by J.C. Chen, Cleveland, Ohio, U.S.A., 89-96.

Tsai, C.S., Chiang, T.C., Chen, B.J. and Lin, S.B. (2003b), "An advanced analytical model for high damping rubber bearings", *Earthq. Eng. Struct. Dyn.*, **32**, 1373-1387.

Tsopelas, P.C., Nagarajaiah, S. and Constantinou, M.C. (1991), "3D-BASIS-M: Nonlinear dynamic analysis of multiple building base isolated structures", Technical Report NCREE-91-0014, State University of New York at Buffalo.

Tsopelas, P.C., Constantinou, M.C. and Reinhorn, A.M. (1994), "3D-BASIS-ME: Computer program for nonlinear dynamic analysis of seismically isolated single and multiple structures and liquid storage tanks", Technical Report NCREE-94-0010, State University of New York at Buffalo.

Wen, Y.K. (1976), "Method for random vibration of hysteretic systems", *J. Eng. Mech. Div.*, **102**(2), 249-263.